Journal of Nuclear Materials 408 (2011) 176–182

Contents lists available at ScienceDirect

Journal of Nuclear Materials

journal homepage: www.elsevier.com/locate/jnucmat

Generalized Kearns texture factors and orientation texture measurement

J.A. Gruber *, S.A. Brown, G.A. Lucadamo

Bechtel Marine Propulsion Corporation, P.O. Box 79, West Mifflin, PA 15122, United States

ARTICLE INFO

Article history:
Received 27 August 2010
Accepted 17 November 2010

ABSTRACT

A generalization of the Kearns texture factors is presented. Mathematical relationships are derived that relate the generalized texture factors to other measures commonly used in quantitative texture analysis. In addition, values of the generalized texture factors for random orientation texture, numerical bounds for the texture factors, and estimates for experimental uncertainty are given. Kearns' method for measuring texture factors from $\theta - 2\theta$ X-ray diffraction scans is extended for use in measuring higher order texture factors. A comparison of generalized texture factors measured through three common experimental techniques is presented.

1. Introduction

The Kearns texture factors are a widely used method for quantifying texture information of hexagonal materials [1]. Their use is especially prevalent in the nuclear industry, with the use of zirconium-based alloys as structural materials and hafnium metal as a thermal neutron poison. The texture factors provide a quantitative way to assign volume fractions of crystallites with (typically) basal poles aligned toward any single sample direction. In particular, for three mutually orthogonal sample directions, the Kearns texture factors necessarily sum to one. This facilitated Kearns' further analysis, in which he used the texture factors in a simple averaging scheme to compute the bulk thermal expansion behavior of Zircaloy [1].

The success of Kearns' thermal expansion model (essentially the same as the Reuss model, see e.g. [2]), as well as the intuitive nature of the texture factors, likely contributed to the further use of the texture factors as a means for quantifying the texture of materials with hexagonal crystal structure. Additionally, Kearns showed how to measure the texture factors using $\theta - 2\theta$ X-ray diffraction scans, an experimental technique which was more widely available at the time than conventional pole figure analysis.

While the simplicity of representation provided by the Kearns texture factors is appealing, it is clear that they contain very limited information about the true orientation texture of a material. Anderson et al. [3] demonstrated that the texture factors are in fact equivalent to the lowest order coefficients of a harmonic expansion of the orientation distribution function [4].

In this document, we introduce a generalization of the Kearns texture factors, motivated by the need for a more complete description of texture while retaining the elegance of Kearns' original work. We develop rigorous mathematical relationships between texture factors and harmonic coefficients of the orientation distribution, and similarly relationships between the texture factors and harmonic coefficients of pole figures and inverse pole figures. We derive relationships between texture factors for different reflecting poles. We also compute higher order texture factors for random orientation texture, numerical bounds for the texture factors, and we discuss estimates for statistical uncertainty in measurement. Finally, we discuss a comparison of generalized texture factors measured through three common experimental techniques.

2. Background

2.1. Kearns texture factors

Kearns defined the texture factor f as a weighted average of the basal pole figure intensity with respect to the sample normal direction. In particular, he defined[1]

$$f \equiv \frac{\int_0^{\pi} I(\vartheta)\cos^2\vartheta\sin\vartheta\,d\vartheta}{\int_0^{\pi} I(\vartheta)\sin\vartheta\,d\vartheta}. \tag{1}$$

Here, $I(\vartheta)$ is the average pole figure intensity at an angle ϑ from the sample normal. The function $I(\vartheta)$ used by Kearns is equivalent to the integral $\int_0^{2\pi} I(\varphi,\vartheta)\,d\varphi$ over the pole figure intensity $I(\varphi,\vartheta)$, which is a function of both spherical angles.

Texture factors are typically measured in three orthogonal sample directions. For tubular material, measurements are most often performed in the longitudinal, transverse, and radial directions. For rolled sheet, the texture factors are usually measured in the rolling, transverse, and normal directions. We adopt the notation used by

[1] Note a slight departure from Kearns' original notation. Additionally, to avoid confusion regarding integration limits, we consider pole figures to be defined over the entire unit sphere.

* Corresponding author. Tel.: +1 412 476 5282.

0022-3115/$ - see front matter © 2010 Elsevier B.V. All rights reserved.
doi:10.1016/j.jnucmat.2010.11.031

Anderson et al. [3] and use the latter convention, whereby the texture factors are labeled f_R, f_T, and f_N, respectively.

2.2. Relation to harmonic coefficients of the orientation distribution function

While the texture factors are a convenient, intuitive way to quantitatively describe the orientation texture of hexagonal materials, it is clear that a set of three numbers, only two of which are independent, do not constitute a complete description of orientation texture. The expansion of the orientation distribution function (ODF) in a series of generalized spherical harmonics is a common way to provide a full characterization of texture [4]. If the texture factors can be related to coefficients of the harmonic expansion of the ODF, then we might answer the question of how much texture information they represent. Recently, Anderson et al. [3] derived expressions relating the texture factors to the harmonic coefficients of the generalized spherical harmonic expansion according to Roe's convention,

$$w(\psi,\theta,\phi)=\sum_{l=0}^{\infty}\sum_{m=-l}^{l}\sum_{n=-l}^{l}W_{lmn}Z_{lmn}(\cos\theta)e^{-im\psi}e^{-in\phi}. \tag{2}$$

The ODF is written as $w(\psi,\theta,\phi)$, and is a function of three Euler angles; the reader is referred to Roe's original article for more details [5]. The constants W_{lmn} are the harmonic coefficients, and the function $Z_{lmn}(x)$ is called the augmented Jacobi polynomial. All conventions for the generalized spherical harmonics used by Roe are retained here. In particular, $w(\psi,\theta,\phi)$ is normalized such that its integral over the full range of Euler angles is one.

Recognizing the equivalence of the inner product of two unit vectors and the cosine of the angle between them, a coordinate free expression for the texture factor along any direction x' can be written as

$$f=\int_A q(x)\langle x,x'\rangle^2 dA, \tag{3}$$

where the integral is taken over the unit sphere and dA is the usual invariant measure. Here, $q(x)$ is the normalized basal pole figure intensity, i.e.

$$q(x)=I_{0001}(x)\Big/\int_A I_{0001}(x)dA. \tag{4}$$

Anderson et al. showed that, in spherical coordinates where $x=x(\varphi,\vartheta)$ and $dA=\sin\vartheta d\vartheta d\varphi$,

$$f_R=\int_0^{2\pi}\int_0^{\pi}q(\varphi,\vartheta)\cos^2\varphi\sin^3\vartheta\,d\vartheta\,d\varphi \tag{5}$$

$$f_T=\int_0^{2\pi}\int_0^{\pi}q(\varphi,\vartheta)\sin^2\varphi\sin^3\vartheta\,d\vartheta\,d\varphi \tag{6}$$

$$f_N=\int_0^{2\pi}\int_0^{\pi}q(\varphi,\vartheta)\cos^2\vartheta\sin\vartheta\,d\vartheta\,d\varphi. \tag{7}$$

For basal poles, the normalized pole figure intensity is related to the ODF in a simple way,

$$q(\varphi,\vartheta)=\int_0^{2\pi}w(\varphi,\vartheta,\phi)d\phi. \tag{8}$$

When combined, the above lead to the result

$$f_R=\frac{4\pi^2\sqrt{2}}{3}W_{000}-\frac{4\pi^2\sqrt{10}}{15}W_{200}+\frac{4\pi^2\sqrt{15}}{15}(W_{220}+W_{2\bar{2}0}) \tag{9}$$

$$f_T=\frac{4\pi^2\sqrt{2}}{3}W_{000}-\frac{4\pi^2\sqrt{10}}{15}W_{200}-\frac{4\pi^2\sqrt{15}}{15}(W_{220}+W_{2\bar{2}0}) \tag{10}$$

$$f_N=\frac{4\pi^2\sqrt{2}}{3}W_{000}+\frac{8\pi^2\sqrt{10}}{15}W_{200}. \tag{11}$$

Because $W_{220}=W^*_{2\bar{2}0}$, each texture factor is real, as expected. [2] Also note that, under the assumption of orthotropic sample symmetry, $W_{220}=W_{2\bar{2}0}$, and the above becomes a system of three linear equations in three unknowns, as shown by Anderson et al. [3]. Solving for the harmonic coefficients gives

$$W_{000}=\frac{\sqrt{2}}{8\pi^2} \tag{12}$$

$$W_{200}=\frac{\sqrt{10}}{16\pi^2}(3f_N-1) \tag{13}$$

$$W_{220}+W_{2\bar{2}0}=\frac{\sqrt{15}}{8\pi^2}(f_R-f_T). \tag{14}$$

For materials with hexagonal crystal symmetry, the only nonzero harmonic coefficients W_{lmn} with $l\leqslant 2$ are those shown here. It is then apparent that the texture factors represent the same texture information as the low order harmonic coefficients of the ODF. In the following section we discuss a generalization of the texture factors, which naturally leads to expressions for the higher order harmonic coefficients.

3. Generalized texture factors

3.1. Definitions

The Kearns texture factor f may be generalized to higher order texture factors $f^{(k)}$ by changing the weighting scheme used in (3),

$$f^{(k)}=\int_A q(x)\langle x,x'\rangle^k dA, \tag{15}$$

where as above, x' is a fixed direction in the sample coordinate system. The generalized texture factors contain no useful information for odd k, i.e. $f^{(k)}=0$, a result of the inversion symmetry inherent in pole figure measurement. When $k=0$, $f^{(0)}=1$ regardless of the chosen sample direction because $q(x)$ is normalized such that its integral is unity. We therefore focus our attention on texture factors with $k\geqslant 2n$, where n is an integer.

For the remainder of this section, it is assumed that $q(x)$ represents the normalized basal pole figure intensity. This definition leads to expressions for $f^{(k)}$,

$$f_R^{(k)}=\int_0^{2\pi}\int_0^{\pi}q(\varphi,\vartheta)\cos^k\varphi\sin^{k+1}\vartheta\,d\vartheta\,d\varphi \tag{16}$$

$$f_T^{(k)}=\int_0^{2\pi}\int_0^{\pi}q(\varphi,\vartheta)\sin^k\varphi\sin^{k+1}\vartheta\,d\vartheta\,d\varphi \tag{17}$$

$$f_N^{(k)}=\int_0^{2\pi}\int_0^{\pi}q(\varphi,\vartheta)\cos^k\vartheta\sin\vartheta\,d\vartheta\,d\varphi. \tag{18}$$

The generalized texture factors with $k=2$ (again, for basal pole figures) correspond to the usual Kearns texture factors, and their relation to the harmonic coefficients W_{lmn} of the orientation distribution has been given in the previous section. For the particular case $k=4$, we evaluate the integrals above to find

$$\begin{aligned}f_R^{(4)}=&\frac{4\pi^2\sqrt{2}}{5}W_{000}-\frac{8\pi^2\sqrt{10}}{35}W_{200}+\frac{8\pi^2\sqrt{15}}{35}(W_{220}+W_{2\bar{2}0})\\&+\frac{4\pi^2\sqrt{2}}{35}W_{400}-\frac{8\pi^2\sqrt{5}}{105}(W_{420}+W_{4\bar{2}0})\\&+\frac{4\pi^2\sqrt{35}}{105}(W_{440}+W_{4\bar{4}0})\end{aligned} \tag{19}$$

[2] The notation W^* indicates the complex conjugate of W.

$$f_T^{(4)} = \frac{4\pi^2\sqrt{2}}{5}W_{000} - \frac{8\pi^2\sqrt{10}}{35}W_{200} - \frac{8\pi^2\sqrt{15}}{35}(W_{220} + W_{22\bar{0}}) + \frac{4\pi^2\sqrt{2}}{35}W_{400} + \frac{8\pi^2\sqrt{5}}{105}(W_{420} + W_{42\bar{0}}) + \frac{4\pi^2\sqrt{35}}{105}(W_{440} + W_{44\bar{0}}) \quad (20)$$

and

$$f_N^{(4)} = \frac{4\pi^2\sqrt{2}}{5}W_{000} + \frac{16\pi^2\sqrt{10}}{35}W_{200} + \frac{32\pi^2\sqrt{2}}{105}W_{400}. \quad (21)$$

As above, all of the nonzero harmonic coefficients for hexagonal crystal symmetry with $l \leqslant 4$ appear in the preceding equations. This result shows that the texture factors of order 4 are linear functions of the harmonic coefficients with $l \leqslant 4$. It happens that this result is true for arbitrary k. The proof of this statement follows from the fact that $\cos^k\vartheta$ and $\sin^k\vartheta$ can both be represented as linear combinations of the associated Legendre functions $P_l^m(\cos\vartheta)$ with $l \leqslant k$. The orthogonality of the associated Legendre functions on $[0, \pi]$ guarantees that only those spherical harmonics with $l \leqslant k$ contribute to the innermost integral in the definition of $f^{(k)}$.

Inverting the previous relations,

$$W_{400} = \frac{3\sqrt{2}}{64\pi^2}\left[35f_N^{(4)} - 30f_N^{(2)} + 3\right] \quad (22)$$

$$W_{420} + W_{42\bar{0}} = -\frac{3\sqrt{5}}{16\pi^2}\left[7\left(f_R^{(4)} - f_T^{(4)}\right) - 6\left(f_R^{(2)} - f_T^{(2)}\right)\right] \quad (23)$$

$$W_{440} + W_{44\bar{0}} = \frac{3\sqrt{35}}{32\pi^2}\left[4\left(f_R^{(4)} + f_T^{(4)}\right) - 3f_N^{(4)} - 6\left(f_R^{(2)} + f_T^{(2)}\right) + 3\right]. \quad (24)$$

For hexagonal materials, the measurement of the usual Kearns texture factors corresponding to the basal pole, along with a similar measurement of $f_R^{(4)}, f_T^{(4)}$, and $f_N^{(4)}$, is therefore sufficient to determine all nonzero harmonic coefficients of order $l \leqslant 4$. This is significant in that commonly used methods for approximating bulk polycrystal properties, such as the Voigt–Reuss–Hill analysis for the elastic stiffness or the thermal expansion tensors, require precisely this texture information [6]. While additional harmonic coefficients may be determined from texture factors of still higher order, we note that the basal pole figure is limited to providing only information about coefficients W_{lmn} with $n = 0$ because of the effective integration over the third Euler angle. When such coefficients are desired, deriving the relationship between generalized texture factors and pole figures for other reflecting poles may provide a solution.

At this point, the utility of the generalized texture factors is likely to be unclear, as they provide no additional information about the orientation distribution of a polycrystal beyond a subset of the harmonic coefficients. This representation, however, lends itself to some unique analysis. Like the usual Kearns texture factors, the generalized texture factors have a more intuitive interpretation than do the coefficients of the harmonic expansion of the ODF. Unlike harmonic coefficients, the generalized texture factors do not depend on a particular choice of convention for the Euler angles or spherical harmonics. They then provide a much simpler means of communicating *numerical* texture information. Finally, the generalized texture factors may be computed quite naturally using a trivial modification to Kearns' original analysis of $\theta - 2\theta$ X-ray diffraction scan data. This allows harmonic coefficients of order $l > 2$ to be derived from $\theta - 2\theta$ scan data as described later.

3.2. Random orientation texture

In the case of random orientation texture, $q(x)$ is a constant equal to $1/(4\pi)$, and the value of the integral in (15) becomes independent of the choice of sample direction. This means that, for fixed k, the texture factors $f^{(k)}$ measured in all directions must be equal. Without loss of generality, we compute $f_N^{(k)}$ for the basal pole figure,

$$f_N^{(k)} = \int_0^{2\pi}\int_0^{\pi} q(\varphi,\vartheta)\cos^k\vartheta\sin\vartheta\,d\vartheta\,d\varphi = \frac{1}{2}\int_0^{\pi}\cos^k\vartheta\sin\vartheta\,d\vartheta = \frac{1}{1+k}. \quad (25)$$

The same value is of course obtained for any other sample directions. Thus for random texture, $f^{(2)} = 1/3$ in all sample directions as originally demonstrated by Kearns, while the higher order texture factors satisfy $f^{(4)} = 1/5$, $f^{(6)} = 1/7$, etc. This result also applies to texture factors corresponding to poles other than the basal pole. This fact may be derived from the general relationship between pole figures and orientation distribution functions (see Eq. (13) of [5]), but may also be surmised from the fact that the assignment of the crystal coordinate system may be chosen arbitrarily.

3.3. Bounds for the generalized texture factors

Bounds for the generalized texture factors may be derived as follows. The normalized pole figure intensity $q(\varphi, \vartheta)$ is a probability density function and therefore takes only positive real values. Likewise, the inner product $\langle x, x'\rangle$ in the definition of $f^{(k)}$ is positive for even k, and so it follows that the integral of their product is non-negative. We also have that $\langle x, x'\rangle \leqslant 1$, and so

$$f^{(k)} = \int_A q(x)\langle x, x'\rangle^k dA \leqslant \int_A q(x)\cdot 1 dA = 1. \quad (26)$$

It then follows that, for any arbitrary sample direction x',

$$0 \leqslant f^{(k)} \leqslant 1. \quad (27)$$

These bounds are attainable, i.e. $f^{(k)} \to 1$ as $q(x) \to \delta(x - x')$, and $f^{(k)} \to 0$ as $q(x) \to \delta(x - x'_\perp)$, where $x'_\perp$ is any direction perpendicular to x'.

3.4. Relation to harmonic expansion of the orientation distribution function

We now derive a general relationship between texture factors and the harmonic coefficients of the ODF. Recall the definition of the texture factor of order k along the sample z axis:

$$f^{(k)} = \int_A q(\varphi,\vartheta)\cos^k\vartheta dA. \quad (28)$$

Note that it has not been assumed that this is the usual sample "normal direction," but rather that in the sample coordinate system used, the texture factor is measured for the z sample direction. It is also unnecessary at this stage to choose a particular pole. Next we consider the Legendre polynomials $P_l(\cos\theta)$ of even order, the first few of which are given by

$$P_0(\cos\theta) = 1 \quad (29)$$

$$P_2(\cos\theta) = \frac{1}{2}(3\cos^2\theta - 1) \quad (30)$$

$$P_4(\cos\theta) = \frac{1}{8}(35\cos^4\theta - 30\cos^2\theta + 3) \quad (31)$$

....

Expressions for Legendre polynomials of higher order can be found in a number of reference works, e.g. [7]. Now, with a slight abuse of notation, we define a function $P_l(f)$ on the set of generalized texture factors, in analogy to the Legendre polynomials, such that in each instance $\cos^k\theta$ is replaced by $f^{(k)}$, e.g.

$$P_0(f) = 1 \tag{32}$$

$$P_2(f) = \frac{1}{2}(3f^{(2)} - 1) \tag{33}$$

$$P_4(f) = \frac{1}{8}(35f^{(4)} - 30f^{(2)} + 3) \tag{34}$$

....

We then combine this with the definition (15) to get

$$P_l(f) = \int_A q(\varphi,\vartheta)P_l(\cos\vartheta)dA. \tag{35}$$

From the definition of the augmented Jacobi polynomial [5],

$$Z_{l00}(\cos\vartheta) = \sqrt{\frac{2l+1}{2}}P_l(\cos\vartheta), \tag{36}$$

and the orthonormality of the spherical harmonics, it may be shown that

$$P_l(f) = 4\pi^2\left(\frac{2}{2l+1}\right)\sum_{n=-l}^{l} W_{l0n}Z_{ln0}(\cos\theta_p)e^{in\phi_p}. \tag{37}$$

The second equality follows from Roe's formula relating the coefficients of the spherical harmonic expansion of pole figures to the generalized spherical harmonic expansion of the orientation distribution function (see Eq. (13) of [5]). Here, ϕ_p and θ_p are the spherical coordinates for the pole. This expression is valid for arbitrary poles, given that the texture factor is measured along the sample z direction, and generates a linear equation relating the texture factors to the harmonic coefficients of the ODF.

The harmonic coefficients so determined, however, correspond to the orientation distribution measured in a particular sample coordinate system. This system may not agree with the our usual choice ($R \to x$, $T \to y$, $N \to z$), and in any case, we want to determine the relationship between the harmonic coefficients and the texture factors measured in any number of directions. For example, when the $f^{(k)}$ are determined from the normal plane, the harmonic coefficients correspond to those of the orientation distribution function in the "standard" sample coordinate system. However, when the texture factor is measured for another plane, the coefficients correspond to the orientation distribution measured in a sample coordinate system rotated with respect to the standard system. It can be shown that the harmonic coefficients W'_{lmn} of the orientation distribution function, given in some rotated sample coordinate system, may be related to the harmonic coefficients W_{lmn} in the standard sample coordinate system by

$$W'_{lmn} = \sqrt{\frac{2}{2l+1}}\sum_{r=-l}^{l} W_{lrn}Z_{lmr}(\cos\theta_s)e^{im\psi_s}e^{ir\phi_s}, \tag{38}$$

where the rotated coordinate system is related to the standard system through a rotation parameterized by the Euler angles ψ_s, θ_s, ϕ_s. Inserting this into the previous equation and swapping indices, we have the general result

$$P_l(f) = 4\pi^2\left(\frac{2}{2l+1}\right)^{3/2}\sum_{m=-l}^{l}\sum_{n=-l}^{l} W_{lmn}Z_{l0m}(\cos\theta_s)e^{im\phi_s}Z_{ln0}(\cos\theta_p)e^{in\phi_p}. \tag{39}$$

This expression relates a linear combination of texture factors to the harmonic coefficients of the ODF. It is completely general, in that it is valid for arbitrary poles as well as arbitrary sample directions. The spherical angles for the pole (ϕ_p, θ_p) are, of course, taken with respect to the crystal coordinate system, while the angles (ϕ_s, θ_s) are spherical coordinates for the direction in which the texture factors are measured, taken with respect to sample coordinates. This expression generalizes the result of Anderson et al. [3] for the usual texture factors, as well as the result derived above for the case $k = 4$.

3.5. Relation to harmonic expansion of pole figures and inverse pole figures

It is also common to express pole figures or inverse pole figures by spherical harmonic expansion,

$$q(\varphi,\vartheta) = \sum_{l=0}^{\infty}\sum_{m=-l}^{l} Q_{lm}P_l^m(\cos\vartheta)e^{-im\varphi}, \tag{40}$$

where $P_l^m(\cos\vartheta)$, the associated Legendre function, is normalized according to Roe's convention, which implies $P_l^m(x) = Z_{lm0}(x)$ [5]. Roe's solution to the pole figure inversion problem,

$$Q_{lm} = 2\pi\sqrt{\frac{2}{2l+1}}\sum_{n=-l}^{l} W_{lmn}P_l^n(\cos\theta_p)e^{in\phi_p}, \tag{41}$$

combined with (39), gives

$$P_l(f) = 2\pi\left(\frac{2}{2l+1}\right)\sum_{m=-l}^{l} Q_{lm}P_l^m(\cos\theta_s)e^{im\phi_s}. \tag{42}$$

This is the relation between the harmonic coefficients of the pole figure and the generalized texture factors. Similarly, the inverse pole figure may be expanded as

$$r(\varphi,\vartheta) = \sum_{l=0}^{\infty}\sum_{n=-l}^{l} R_{ln}P_l^n(\cos\vartheta)e^{-in\varphi}, \tag{43}$$

and is related to the harmonic coefficients of the ODF by [2]

$$R_{ln} = 2\pi\sqrt{\frac{2}{2l+1}}\sum_{m=-l}^{l} W_{lmn}P_l^m(\cos\theta_s)e^{im\phi_s}, \tag{44}$$

which leads to

$$P_l(f) = 2\pi\left(\frac{2}{2l+1}\right)\sum_{n=-l}^{l} R_{ln}P_l^n(\cos\theta_p)e^{in\phi_p}. \tag{45}$$

3.6. Relationships between texture factors for different poles

Here we use the result (37) to derive a few relations between texture factors for different poles. In particular, we are able to rigorously derive the relationships found by Kearns through more heuristic arguments [8].

In the particular case $l = 2$, (37) reduces to

$$P_2(f_{hkil}) = \frac{4\pi^2\sqrt{10}}{5}W_{200}P_2(\cos\theta_p), \tag{46}$$

where the reflecting pole is labeled ($hkil$). For basal pole figures, $\theta_p = 0$ and so $P_2(\cos\theta_p) = 1$. Combining this with the previous relationship,

$$P_2(f_{hkil}) = P_2(f_{0001})P_2(\cos\theta_p). \tag{47}$$

Rearranging and simplifying gives

$$f^{(2)}_{hkil} = \frac{1}{2}\left[f^{(2)}_{0001}(3\cos^2\theta_p - 1) + \sin^2\theta_p\right], \tag{48}$$

which is precisely the relationship suggested by Kearns (Eq. (6) of [8]). Note that, while this relationship holds for arbitrary sample directions, the texture factors all correspond to measurements made in the *same* sample direction.

A similar relation may be derived for the case $l = 4$. Now we have, in the general case,

$$P_4(f) = \frac{4\pi^2\sqrt{2}}{3}W_{400}P_4(\cos\theta_p), \tag{49}$$

and substitution of $P_4(f_{0001})$ gives

$$P_4(f_{hkil}) = P_4(f_{0001})P_4(\cos\theta_p), \tag{50}$$

which again holds for arbitrary sample directions.

3.7. Kearns factors and statistical uncertainty

In practical applications, it is useful to know the statistical uncertainty associated with computing texture factors from a limited data set, i.e. a small number of grains. Here we note that each texture factor $f^{(k)}$ may be considered as the expectation value of a random variable $\xi^k \equiv \cos^k\theta$, where θ is the angle between the measurement (sample) direction and the reflecting pole. The probability density $p(\xi)$ depends on the texture itself. Likewise the uncertainty also depends on the texture, but it is possible to derive a conservative estimate by assuming that random texture (uniform $p(\xi)$) leads to the largest possible statistical variance. Making use of (25), the variance is

$$\sigma^2 = \int_{-1}^{1}\left(\frac{1}{1+k} - \xi^k\right)^2 p(\xi)d\xi = \frac{k^2}{(1+k)^2(1+2k)}. \tag{51}$$

We can then compute confidence intervals for the texture factors as [9]

$$f^{(k)} \pm \frac{z_{\alpha/2}k}{(1+k)\sqrt{(1+2k)N}}. \tag{52}$$

As a simple test, we computed the standard deviation σ associated with measuring $f^{(k)}$ from a set of N randomly generated orientations (Fig. 1). The simulated data is in good agreement with the analytical result. We also give, in tabulated form, the number of grains necessary to compute $f^{(2)}$ within a given interval and confidence level (Table 1).

In situations where (51) is overly conservative, e.g. for highly textured samples, it is still possible to compute approximate error bounds using a straightforward Monte Carlo calculation. In this approach, N orientations would be generated with probabilities dictated by the measured texture, and the standard deviation in the computed Kearns factors would be recorded. Note that, by using this "bootstrapping" procedure, it is assumed that the measured texture is a reasonable approximation of the true texture.

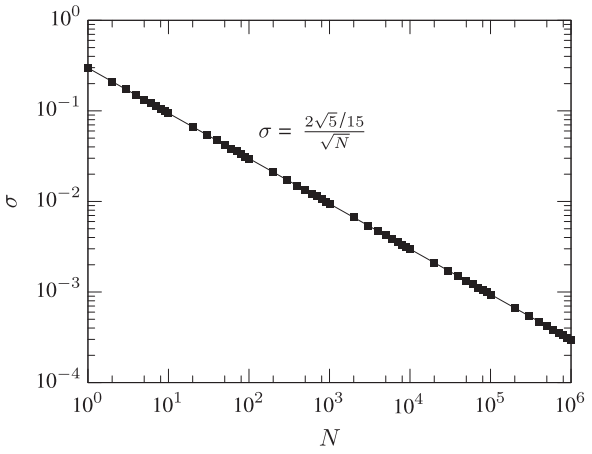

Fig. 1. Standard deviation σ associated with texture factor $f^{(2)}$ for a random orientation texture as a function of number of grains N. Points indicate averages over 50 simulations, while the line indicates the analytical solution given in the text.

Table 1
Number of grains necessary to determine texture factor $f^{(2)}$ within a given numeric interval for various confidence levels.

	90%	95%	99%
$f \pm 0.1$	16	25	49
$f \pm 0.05$	81	121	225
$f \pm 0.01$	2401	3364	5776
$f \pm 0.005$	9604	13,456	23,409
$f \pm 0.001$	240,100	341,056	589,824
$f \pm 0.0005$	962,361	1,366,561	2,359,296
$f \pm 0.0001$	24,078,649	34,187,409	59,043,856

3.8. Measurement of generalized texture factors by $\theta - 2\theta$ X-ray diffraction

Here we provide a brief overview of the method for computing texture factors from $\theta - 2\theta$ X-ray diffraction scans, as used by Kearns [1]. The extension of the method to measuring generalized texture factors involves a trivial modification of Kearns' procedure.

Conventional $\theta - 2\theta$ scans produce a discrete set of intensities for given families of diffracting planes. In hexagonal materials, these planes take the form $(10\bar{1}l)$, $(21\bar{3}l)$, and $(11\bar{2}l)$. Kearns defined $I_1(\vartheta)$ as the intensity of the pole figure with fixed $\varphi = 0^\circ$. This function is approximated by a linear interpolation of intensity data from the family of $(10\bar{1}l)$ poles. The functions $I_2(\vartheta)$ and $I_3(\vartheta)$ correspond to the pole figure intensity at $\varphi = 19.1^\circ$ and $\varphi = 30^\circ$, respectively. These are similarly approximated by intensities from $(21\bar{3}l)$ and $(11\bar{2}l)$ poles, respectively. The function $I(\vartheta)$ appearing in Kearns' definition of the texture factor (1) is then determined by a suitable interpolation using various combinations of I_1, I_2, and I_3, depending on the range of ϑ, e.g. for zirconium, Kearns used

$$I(\vartheta) = \frac{1}{30}\left[19.1\left(\frac{I_1(\vartheta)+I_2(\vartheta)}{2}\right) + 10.9\left(\frac{I_2(\vartheta)+I_3(\vartheta)}{2}\right)\right] \times 58.3^\circ \leqslant \vartheta \leqslant 90^\circ. \tag{53}$$

Details regarding the interpolation scheme are given in the original reference [1]. Note that the appropriate ranges depend on the c/a ratio for the material under consideration.

Using this definition of $I(\vartheta)$, Kearns then computed texture factors by numerical integration of (1) over discrete intervals. In doing so, at each value of ϑ, the intensity $I(\vartheta)$, the weighting factor $\cos^2\vartheta$, and the discrete area element $\sin\vartheta\,\Delta\vartheta$ are all computed. Clearly, the same procedure may be used to compute generalized texture factors of any order k by simply replacing the weighting factor $\cos^2\vartheta$ with $\cos^k\vartheta$.

While the numerical integration may easily be performed to any accuracy desired, it should be noted that any method for interpolating the function $I(\vartheta)$ from a discrete set of intensities will introduce errors into the calculation that are difficult to quantify. It is not known *a priori* whether Kearns' method will be appropriate for any particular specimen; it is quite possible that there are orientation textures for which this method will produce poor results. Our extension to the method suffers from the same limitation. However, we will later demonstrate an instance where generalized texture factors measured from $\theta - 2\theta$ scans compare well with those determined by other methods.

4. Experimental

4.1. Sample preparation

For X-ray diffraction experiments, two Zircaloy-4 specimens measuring 0.5 in. × 0.5 in. × 0.125 in. were mounted, ground, and polished using standard metallographic procedures. This surface condition was found to be inadequate for EBSD analysis, so a third

unmounted sample was prepared using an electropolishing technique. The specimen was electropolished using a Struers Lectropol unit with the following conditions: 20% perchloric acid, 80% methanol solution; 15 °C; 13–14 V operating voltage, 1.0–1.2 A current. A 30 s polishing step was followed by a 45 s polishing step for a total electropolishing time of 75 s. All samples were nominally processed in the same way.

4.2. Electron backscatter diffraction (EBSD)

EBSD maps were obtained on an FEI XL-30 field emission gun environmental scanning electron microscope (FEG-ESEM). Orientation maps of a total of 15 areas measuring 400 μm × 300 μm in size distributed over the surface of the polished area were acquired with an HKL EBSD system equipped with a Nordlys S camera and using an accelerating voltage of 20 kV and spot size of 6 at 300× magnification. A pattern was acquired every 2 μm resulting in 30,000 points per map. The average percentage of indexed points within an individual scan was 92%, with standard deviation of 1.1%. Only indexed points were used in the texture factor calculation; no noise correction procedures were used. The total number of grains appearing in the combined scans was estimated to be 9114. The average grain size was measured as 15.2 μm.

For the present analysis, only the angle of the basal pole to the sample normal is needed. Orientation data was collected and reported as Euler angles according to Bunge [4]. With this convention, the generalized texture factor $f^{(k)}$ is simply the average value of the cosine of the second Euler angle, Φ, taken over all measured points.

4.3. X-ray diffraction (XRD) pole figures

Texture measurements were performed using Cr Kα X-ray radiation on a PANalytical high-resolution diffractometer (MRD) equipped with parallel beam optics, Eulerian cradle, and a proportional detector. Instrument verification was done by measuring the (2 1 1) peak position from a randomly oriented tungsten powder at $y = 0°$ and $y = +85°$. The maximum peak shift was 0.006° 2θ which indicates that the instrument is properly aligned for texture measurement. The samples were mounted onto the XYZ stage using double sided tape. The samples were scanned from 30° to 106° 2θ to determine precise peak positions. The (0002), $(10\bar{1}0), (10\bar{1}1), (10\bar{1}2), (10\bar{1}3)$, and $(11\bar{2}0)$ pole figures were measured using a 5° × 5° grid up to a maximum tilt of 85°. A 5 mm beam was used and the samples were oscillated 5 mm in the x and y directions during the measurement. Based on the grain sizes observed with EBSD, it is estimated that about 9×10^5 grains contributed to the pole figure measurement.

The pole figures were analyzed using XPert Texture software from PANalytical. The scans were corrected for background and defocusing. The ODF was calculated assuming hexagonal crystal symmetry and orthorhombic sample symmetry using the texture software by the WIMV method. Complete pole figures and inverse pole figures were calculated from the ODF. Texture factors were determined from the calculated pole figures by numerical integration.

4.4. $\theta - 2\theta$ X-ray diffraction

The samples were run from 30° to 148° 2θ using Cu Kα X-ray radiation on a PANalytical Multipurpose Diffractometer (MPD) configured with a 1/4° divergence slit, 10 mm beam mask, a multipurpose stage, 1/2° anti-scatter slits, and an X'Celerator detector. Instrument verification was done using LaB_6 powder (NIST SRM 660a) by comparison of the observed diffraction peaks with the reference pattern obtained from the ICDD database. Since the sample could not be spun during the analysis, the sample was rotated 90° and reanalyzed. The net intensities from the two diffraction scans were then averaged. Taking into account the beam size and penetration depth (20 μm), the number of grains contributing to this analysis is estimated to be on the order of 2×10^5.

The $\theta - 2\theta$ scans were analyzed using X'Pert HighScore software from PANalytical, Inc. Briefly, the background was subtracted, the pattern was smoothed, and the peaks were fit using a Pseudo-Voigt profile function. The measured intensities were input into a spreadsheet which then calculates the texture factor based on the inverse pole figure method described above.

4.5. Comparison

The generalized texture factors (normal direction, basal pole) were measured up to order 12 by the two X-ray diffraction methods and by EBSD, Tables 2 and 3. It can be seen that the texture factors derived from $\theta - 2\theta$ scans and X-ray pole figures are in good agreement, with typical variations for a given specimen on the order of 2%. In fact, the variation associated with using different methods appears to be of the same magnitude as the variation of the two samples. We then conclude that each of the X-ray diffraction techniques gives equivalent results.

The results from EBSD compare well with the X-ray diffraction methods. It can be seen that the generalized texture factors obtained from EBSD are consistently higher than those from either X-ray diffraction method, albeit only slightly. It is expected that measurements performed on different locations of the same sample will exhibit slight variations in texture. The difference between the texture factors calculated from EBSD scan data and the X-ray

Table 2
Measured generalized texture factors (basal pole) along the sample normal direction. Left column indicates the result of $\theta - 2\theta$ scans, middle column are results derived from X-ray pole figure measurements, and right column is derived from electron backscatter diffraction.

Sample	$f^{(2)}$			$f^{(4)}$			$f^{(6)}$		
1	0.653	0.640	0.655	0.502	0.490	0.504	0.408	0.399	0.411
2	0.649	0.649	–	0.498	0.502	–	0.405	0.410	–

Table 3
Measured generalized texture factors (basal pole) along the sample normal direction. Left column indicates the result of $\theta - 2\theta$ scans, middle column are results derived from X-ray pole figure measurements, and right column is derived from electron backscatter diffraction.

Sample	$f^{(2)}$			$f^{(4)}$			$f^{(6)}$		
1	0.344	0.336	0.348	0.297	0.290	0.301	0.261	0.254	0.265
2	0.341	0.347	–	0.294	0.300	–	0.258	0.263	–

diffraction methods remains within the expected error bounds based on the total number of grains and the analysis described above.

5. Conclusions

We have developed a generalization of the Kearns texture factors and have elaborated on a number of their properties. In particular, we derived mathematical relationships between the generalized texture factors and other measures commonly used in quantitative texture analysis. We have also provided numerical bounds for the texture factors and have discussed estimates for experimental uncertainty. Kearns' method for measuring texture factors from $\theta - 2\theta$ X-ray diffraction scans has been extended for use in measuring higher order texture factors. Generalized texture factors measured through three different experimental techniques are shown to provide comparable information given the measurement uncertainty.

References

[1] J.J. Kearns, Thermal expansion and preferred orientation in Zircaloy, WAPD-TM-472, 1965.
[2] U.F. Kocks, C.N. Tome, H.R. Wenk, Texture and Anisotropy: Preferred Orientations in Polycrystals and their Effect on Materials Properties, Cambridge University Press, Cambridge, UK, 1998.
[3] A.J. Anderson, R.B. Thompson, C.S. Cook, Met. Mater. Trans. A 30 (1999) 1981–1988.
[4] H.J. Bunge, Texture Analysis in Materials Science, Butterworths, London, 1982.
[5] R.J. Roe, J. Appl. Phys. 36 (1965) 2024–2031.
[6] C.M. Sayers, J. Nucl. Mater. 144 (1987) 211–213.
[7] M. Abramowitz, I.A. Stegun, Handbook of Mathematical Functions, National Bureau of Standards, 1968.
[8] J.J. Kearns, J. Nucl. Mater. 299 (2001) 171–174.
[9] I. Miller, J.E. Freund, R.A. Johnson, Probability and Statistics for Engineers, Prentice Hall, Englewood Cliffs, New Jersey, 1990.